Iraqi Journal of Natural Sciences and Nanotechnology IJNSN
Journal Homepage : https://publications.srp-center.iq/index.php/ijn

Uptake of Trivalent Chromium from Simulated Wastewater Using Activated Carbonation of Date Pit Sorbent, Kinetics, and Material Characterization

Basmalh J. Adnan* **and Hayder M. Rashid**

Department of Environmental, College of Engineering University of Baghdad, Baghdad, Iraq.

Corresponding Author: basmala.adnan1611@coeng.uobaghdad.edu.iq

Keywords:

Trivalent chromium; adsorption; kinetics; date pit.

Abstract

The objective of the current investigation is to determine if it is feasible to capture and stabilize chromium ions in simulated wastewater utilizing trash in the form of date pits. The beginning pH range (3-6), initial pollutant concentration (25-125 mg/L), sorbent dosage (0.5-2) g, and agitation speed (50-250 rpm) were among the examined batch balance parameters. At a pH of 6, a toxin concentration of 25 mg/L at first, and an agitation speed of 250 rpm, the maximum contaminant elimination efficiency of (95%) was attained. For Cr (III) removal with activated carbonation of date pit (ACDP) adsorbent, the sips model was found to be the most fitted isotherm model during batch experiments with a corresponding factor R2 of (0.9996). Kinetic outcomes exposed an acceptable contract among the theoretical and experimental results; the findings were close-fitted with the kinetic model of pseudo-second-order which means that the dominant mechanism during the sorption process is a chemisorption.

Introduction

Treatment of wastewater streams from toxic metal ions is an extremely necessary and extensively studied research area [1]. One of the most dangerous contaminants is chromium (Cr). For this metal, there are two oxidation states: Cr(III), which is found in nature and is less dangerous because of its low solubility, and Cr(VI), which is the most widely used industrially and more hazardous to living and environment things owing to its high solubility, mobility, and the oxidizing power [2]. Chromium is a highly desirable industrial metal which is used in a wide variety of applications, including mining, textiles, electroplating, tanning, photography, ceramics, and so on. However, its liquid waste poses potential risks and risks to human health and the surrounding environment [3]. The ions of chromate and dichromate simply pass through the cell membranes and oxidize biological components. Additionally, exposure to these compounds over an extended period may result in ulcers, diarrhea, and eye discomfort [4]. Several chemical and physicochemical treatments have been developed to eliminate chromium ions from

industrial wastewater to protect the humans and environment. Additionally, these treatments allow the possibility of reuse of this water, particularly in arid climate countries. The technologies include reduction followed by chemical precipitation [5-6], ion exchange [7-8], membranes [9-11], electrodeposition [12], electrocoagulation [13], and adsorption [14-22]. The sorption process is the most common and simplest procedure. This method is used for powders or granular materials, especially activated carbon (AC). The application of this method is constrained by the production and regeneration price of sorbents. Interest has recently increased in obtaining inexpensive sorbents (biosorbents, biochar, AC, etc.) from reutilizing industrial by-products or wastes. [23-33]. The goal of the study is to 1) evaluate the efficiency of date palm pits in removing Chromium (III) ions from the electroplating wastewater synthesized. 2) Study the effect of parameters on the adsorbents such as (particle size, initial concentration, pH, agitation speed, and dose of sorbent). 3) dealing with different isotherm models of adsorption (Langmuir, Freundlich, spis, toth, and Temkin), in addition to the Kinetic model such as pseudo-first-order and pseudo-second-order that will be examined to recognize the more fitted one with results data.

Experimental procedure

1. Materials

Waste of date pits (DP) was collected from some local orchards located in Al-Najaf Governorate, where the waste was placed in a large beaker and washed with a 0.1 M HCl solution for 10 minutes. In turn, it washed in batches with distilled water to get rid of all the suspended dust on the outside of the date pits, then it was dried for 4 hours. It was then ground, and the crushed material was soaked in H3PO4 solution for 24 hours, then dried for 24 hours at a temperature of 110 °C, and then burned and activated at a temperature of 650 °C for 2 hours. It was separated using a sieve with a diameter of 250 µm, and it was used for processing. The simulated chromium solution was made by dissolving 7.673 g of hydrated chromium nitrate Cr(NO3)3.9H2O in 1000 ml of deionized water and storing it at room temperature (25°C). To obtain different pH values (3-6), the synthesis solutions' pH was adjusted with 0.1 M NaOH or 0.1 M HCl.

2. Batch tests

Based on batch experiments conducted at a constant temperature, it was determined how the beginning pH, initial concentration (Co) of Cr(III), dose sorbent, particle size sorbent, and agitation speed affected the elimination of this contaminant. Sorbent dosages of, 0.50, 1.5, and 2 g ACDP/ 100 mL were added to flasks of 250 mL containing 100 ml of a trivalent chromium solution of 250 mg/L. The containers were shaken using a (Edmund Buhler SM25, German) shaker with agitation rates ranging from (50-250) rpm and interaction times that vary from (15-90) min. To measure the remaining heavy metal content in the

aqueous solution, a 50mL aliquot was taken out and filtered. AAS flame (type Shimadzu, Japan) was used to detect the concentration of dissolved metal ions in a sample of 10 ml of filtrate.

The percentage R (%) of chromium ions retention and adsorbed mass in equilibrium phase qe (mg/g) are attained from the following equations respectively: The number of metal ions maintained in the solid phase, q_e was determined using the following formula [34]:

$$q_e = (C_o - C_e)\frac{V}{m} \quad (1)$$

$$R = \frac{Co - Ce}{Co} \times 100 \quad (2)$$

Where Co represents the inlet concentration of heavy metal, Ce represents a concentration of heavy metals at equilibrium, V denotes the flask solution volume (L), and m is the sorbent dosage (g).

Results and discussion

1. Initial Contaminant Concentration

The initial solute concentration has a crucial role in the adsorption process. Removal percent (%R) and adsorption uptake (qe) of these contaminants on activated carbon were both affected by the starting concentration of Cr (III), as shown in (figure 1) revealing a marginal drop in chromium ion removal efficiency onto the date pits as the inlet Cr (III) concentration raised from 25 to 125 mg/L with an optimal removal percent of 76%; as well. This figure displayed a speedy drop in removal efficiency of chromium ion until 59%. The greater the driving force, the lengthier the mass transfer path from bulk solution to sorbent surface, which occurs naturally at higher concentrations, which may be the cause of the decrease in removal efficiency.

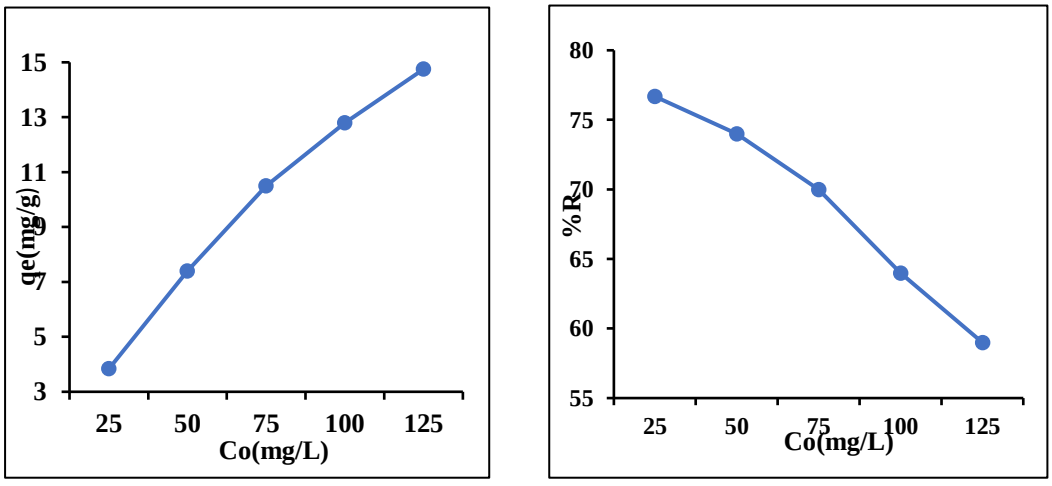

(a) (b)

Figure (1): The Initial Concentration effect of Cr (III) adsorption onto AC, pH of the Contaminated Solution Original, Sorbent dose: 0.5 g/L, Agitation Speed: 250 rpm; Partical Size:1.1 mm, T: (25°C. (a) Adsorption Capacity (b) Removal Efficiency of Adso

2. Effect of particle size

The particle size at sieves (250 µm, 600 µm, and 1 mm) for date pits local adsorbent was evaluated for its effect on the removal effectiveness and sorption capacity (qe) when the factors represented initial concentration (25 mg/L), and pH of the contaminated solution original, sorbent dose (0.5 g/L), rpm (250) at the constant time (60 min) and room temperature from the previous set of experiments as shown in figure (2).

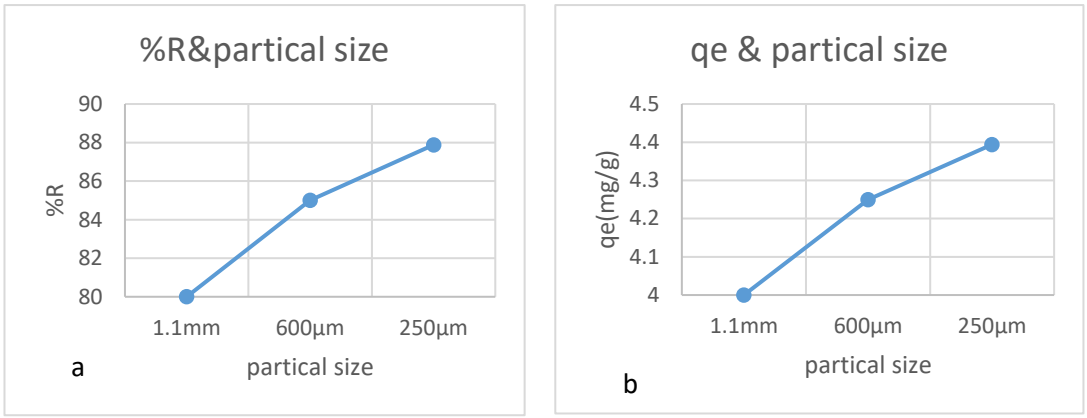

(a) (b)

Figure (2): Particle Size effect on Cr (III) Adsorption onto AC, Co(25 mg/l), Sorbent dose (0.5 g/L), Rpm (250), Constant Contact Time(60 min) at Room Temperature. (a) Removal Efficiency of Adsorption (b) sorption Capacity

As shown in figure (2), a decrease in the sorption percentage with an increase in the particle size of the adsorbents was obtained. This decrease was qualified to a decline in the adsorbent surface area at larger particle sizes which provided less activity to be utilized for the sorption of date pits [36]. Consequently, adsorbents were utilized at a particle size of 250 µm when the effects of other experimental parameters were studied to achieve an optimum adsorption.

3. Effect of PH

PH is the furthermost vital variable in batch experiments method that has a great effect on heavy metal elimination studies. Chromium ions sorption onto date pits was examined with a different pH value (3-6) matching with (25 mg/L) inlet concentration of contaminant and sorbent particle size of (250 µm), sorbent dose (0.5 g/L), Agitation Speed (250 rpm), constant connection times (60 min) with a temperature of about 25◦C. The pH value was altered by adding 0.1 M sodium hydroxide and Hydrochloric acid in small droplets as shown in figure (3).

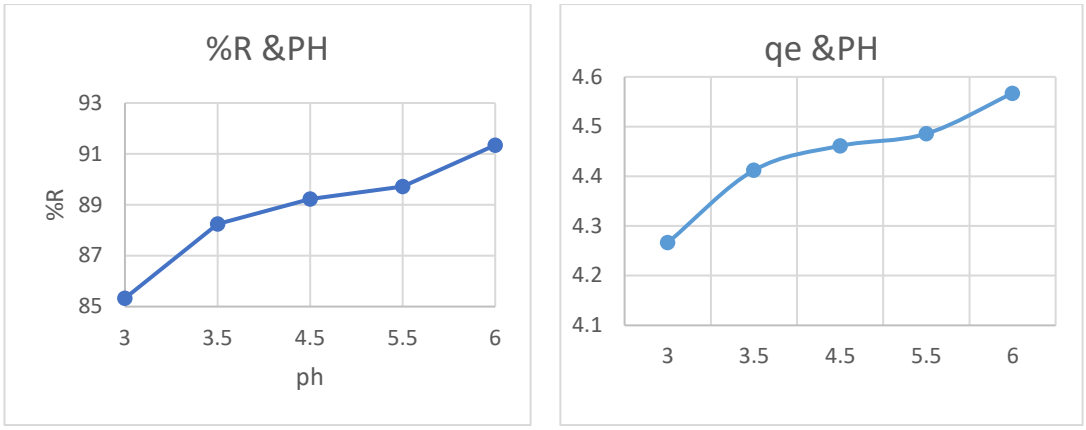

(a) (b)

Figure (3): shows the PH effect on Cr (III) adsorption onto AC, (a) Removal Efficiency of Adsorption (b) Adsorption Capacity have exposed that the optimal chromium ions sorption in ACDP was achieved at a pH value of approximately 6 with a yield removal efficiency of 91.344%.

More hydrogen cations are produced at lower pH levels, in the range of 3 to 4, and this is an illustration of cationic Cr (III) competition with H+ over the sorbent surface. Competition will eventually make it more difficult for pollutants to adhere to the solid phase, which would lower the effectiveness of removal. Precipitation in the form of hydroxides may occur at pH values greater than 6, adhering to the Cr (III) ions' sensitivity to form flocs and hydroxides due to their low solubility at high pH. Similarly, at pH levels above 4, no additional hydrogen cations predominate and no competition for active sites exists; the absorption rates rise and an appropriate removal efficiency is achieved [37].

4.The effects of interaction time

Figure 4 shows the time influence of Cr (III) exposure to the synthesized ACDP in current research during the sorption process. Adsorption was improved in an extended period, and the Cr (III) removal percentage (fixed at 25 ppm, pH 6, 0.5 g/L dosage, and particle size was 250 µm) was 91% after 90 min of interaction. Pore availability was significantly higher in the first few minutes, then gradually decreased. Other batch experiments at this contact time were completed later.

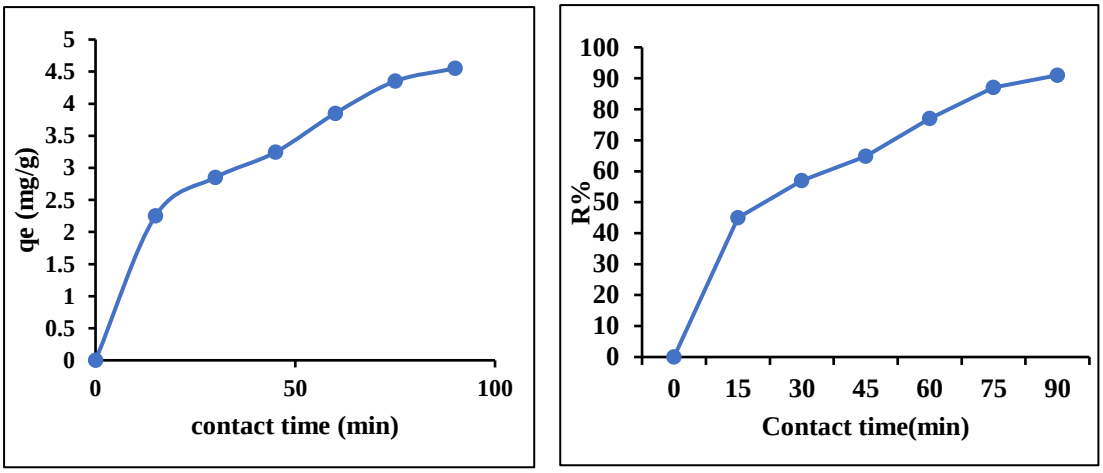

(a) (b)

Figure (4): The Interaction Time effects on Cr (III) Adsorption onto AC, (a) Adsorption Capacity (b)Removal Efficiency of Adsorption.

5. Agitation Speed

The effect of varying agitation speeds (50-250) rpm on chromium ion removal efficiency at constant experimental variables was investigated; 6 pH, 25 mg/L initial contaminant concentration (0.5 g/L) sorbent dose, (250 µm) Sorbent of atomic size and contact time of 60 minutes. In Figure 5, the removal effectiveness of chromium increased exponentially from 50 speed, which corresponded to 69% chromium removal, to 250 rpm, which corresponded to 92% removal percent.

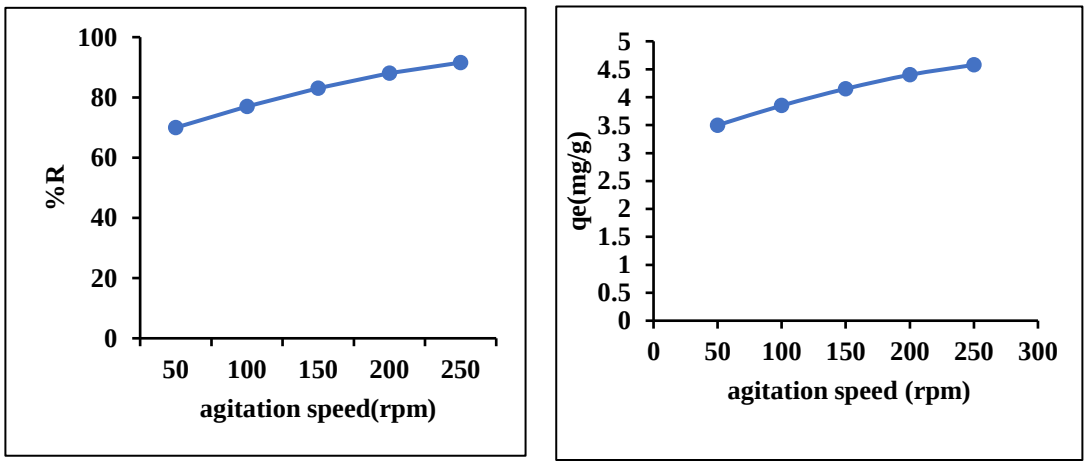

(a) (b)

Figure (5): the Agitation Speed on Cr (III) Adsorption in AC, (a)Removal Efficiency of Adsorption (b) Adsorption Capacity

Increasing agitation speed means a speedy movement of metal ions toward active sites of ACDP, which is the explanation for why the removal efficacy increases as the rpm impaired to the mass-liquid medium increases. This is due to the decreasing diffusion layers that can be converted to resist contaminant migration to the solid phase, and the thickness of this film may be reduced or even eliminated as the agitation speed increases.

6. Effect of Sorbent Dose

The sum of date pits grams for each 100 ml of ion solution was considered to learn the sorbent mass effect on the removal efficiency at constant variables of (6) pH, (25 mg/L) initial concentration of contaminants, particle size sorbent (250 µm) and (250 rpm) agitation speed. In this case, chosen sorbent masses varied range between (0.5-2) g ACDP per 100 ml of an aqueous solution as shown in figure (6).

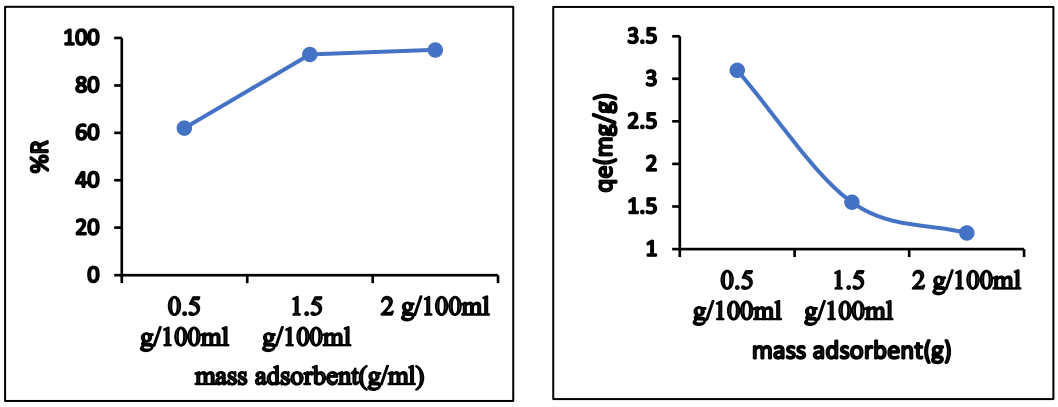

(a) (b)

Figure (6): Effect of Sorbent Mass on the Adsorption of Cr(III) onto Activated Carbon, (a)Removal Efficiency of Adsorption (b) Adsorption Capacity.

The presence of a constant concentration of chromium can be used to describe this. The increasing of AC amount, and consequently the number of available active sites, promotes well Cr (III)ions removal down to a value matching the level limited with the initial concentration of Cr(III). in contrast to, the adsorption uptake (qe=Cads/m) declines with the adsorbent mass increasing.

7. Characterization of the Adsorbents

7.1. Scanning Electron Microscopy (SEM)

A scanning electron microscope (SEM) is an electron microscope that generates images of the surface of a material by inspecting it with a focused beam of electrons. The interaction of electrons with atoms in the adsorbent produced a slew of signals containing information about the sample surface's topography and structure [38,39]. SEM realized on raw and activated date pits are displayed in figure (7). The investigation of the row date stones structure (Figure 7.a) shows the attendance of limited macropores of several sizes and geometry on the sorbent surface. It has been noticed that the activation process added more pits and pores to the adsorbent surface (Figure 7.b), and also there is an extensive

variety of sizes and shapes of intragranular pores. These sorbents have a moderately high porosity due to a combination of irregular grain size and shape, in addition to a great quantity of intragranular porosity, signifying high surface areas. In contrast, the interaction of chromium particles with the adsorbent surface led to additional soft granular volumes in the medium.

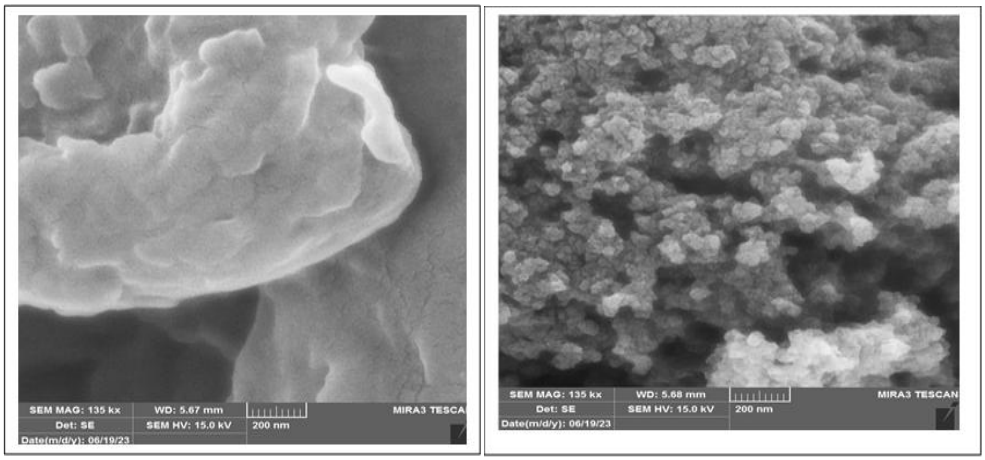

(a) **(b)**

Figure (7): SEM Images for The Date Pits Sorbents before (a) and after (b) the association with Cr (III).

7.2. Surface Area and Pore Volume (BET)

Analyses were conducted to evaluate the prepared date pits' porosity and textural properties. Brunauer-Emmett-Teller (BET) technique is used to measure the surface area of any adsorbent. The results of the BET analyses showed that the surface area of date pit (DP) powder before and after activation was (5.0097) DP and (330.80) ACDP. This increase in the area of ACDP indicates the activation of the date pit (DP), which leads to an improvement in its adsorption capacity [40].

The International Union of Pure and Applied Chemistry (IUPAC) classifies pores into three main groups based on their size: micropores (pore diameter < 2 nm), mesopores (2 nm < pore diameter < 50 nm), and macropores (pore diameter > 50 nm). The mean pore diameter of ACDP was found to be 8.2925 nm, which is within the range of the size of the mesopores. A value of 0.6858 cm3 /g representing the quantity of nitrogen adsorbed at P/P0 of 0.990 was regarded as the total pore volume of ACDP. It becomes more challenging to measure the pore diameter precisely at higher P/P0 values [41].

Table 1: BET analysis for date pits before and after activation.

Analysis demands	DP	ACDP
Surface area (m2/g)	5.0097	330.8
Pore volume (cm^3/g)	0.005922	0.6858
Mean pore diameter (nm)	4.7287	8.2925

7.3 Fourier transform infrared spectroscopy (FT-IR)

Peaks in a sample relate to the various vibrations of the sample's atoms whenever placed under the infrared wavelengths of the electromagnetic spectrum [2] [42]. The middle range IR wavenumber is plotted on the infrared spectrum between 4,000 and 400 cm-1. Figure (8) depicts the situation before

treatment. A spectral band of 3448 and 3417 cm-1, corresponding to O-H of bonded hydrogen, is observed, indicating the attendance to alcohol. The vibrations at 2928 and 2828 cm-1 were caused by symmetric and asymmetric C-H stretch of alkanes, signifying C and H occurrence in date seeds. C=O carbonyl stretching vibration at 1745 cm-1 is found in esters, aldehydes, ketones, and carboxyl groups. Stretch vibration at 1456 cm-1 is owing to O-H bands of the carboxylic acid. 1074 cm-1 peak owing to stretching of C-O of cellulose and hemicellulose found in cell walls. Besides cyclic C-O-C groups coupled to C=C-O-C double carbons in olefinic or aromatic structures that characterize major components of the lignocellulosic material, vibrations at 1292 and 877 cm-1 associated with esters such as CH3CO-O-. 669-511 cm-1 spectral stretch is qualified to vibration of aromatic (C-H) substitution [43,44,45].

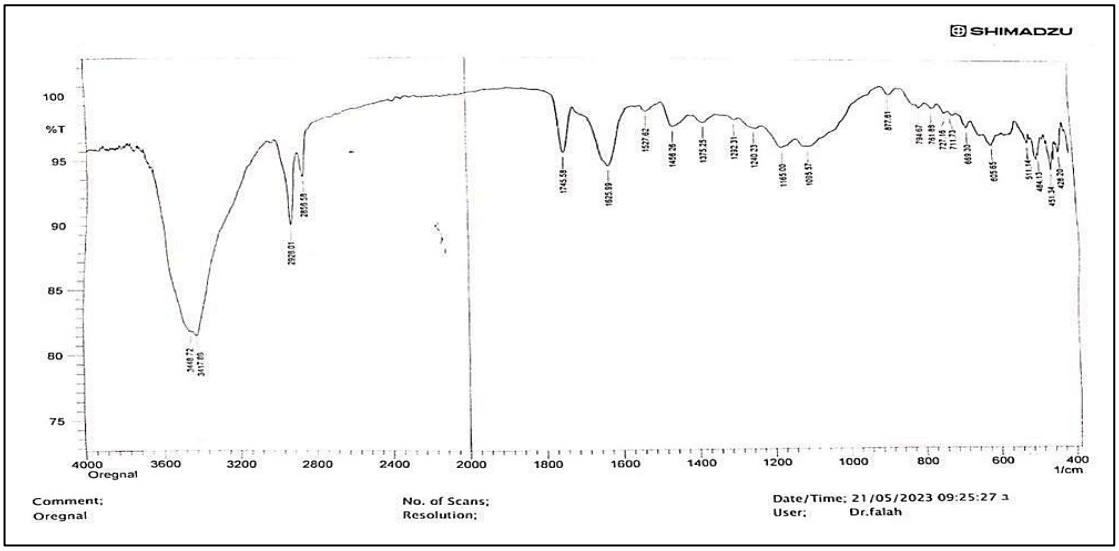

Figure (8): FTIR analysis peaks of row date pits.

Figure (9) illustrates the FTIR spectra of the activated date pits. The most common functional groups discovered were O-H stretching vibrations of hydroxyl functional groups, as well as hydrogen bonding that was noticed at a bandwidth of around 3427 cm-1. Further main peaks noticed were found at the band of 2091-2788 cm-1 giving an indication of C=H stretch which associated alkanes and alkyl groups [46]. Moreover, additional peaks appeared at 1571, 1190, 1147, and 1083 cm−1, which match to stretch of C=O of aliphatic ketone, stretch C=C to conjugated alkene, N–O asymmetric extending owing to nitro compound, O–H bending of carboxylic acids, and S=O stretching of sulfonate [47]. FTIR was used the identify the date seed powder functional groups before and after adsorption.

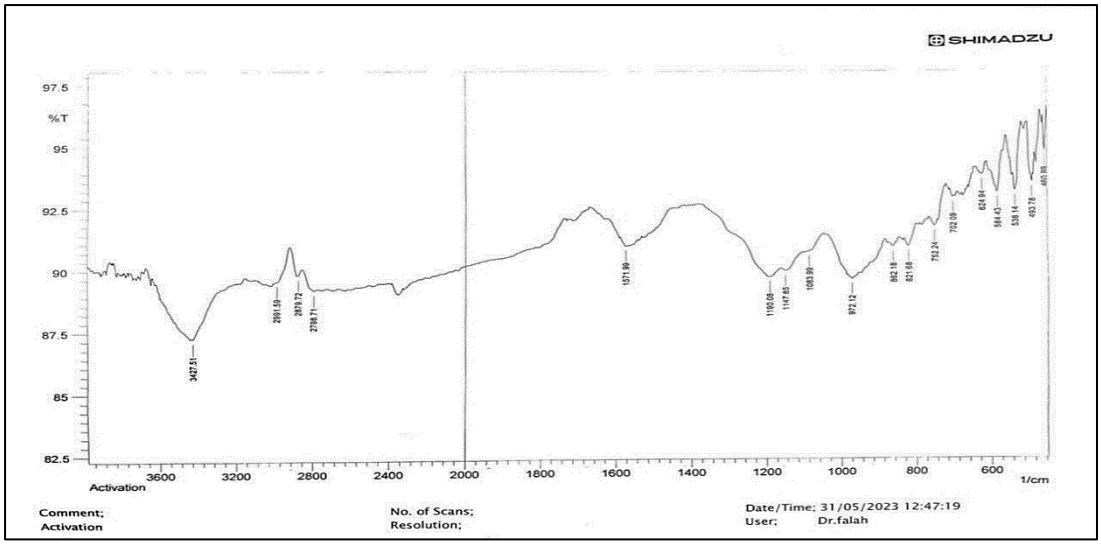

Figure(9): FTIR analysis peaks of activated date pits before Cr(III) adsorption

Figure (10) FTIR analysis of the activated date seed powder after treatment. Following Cr (III)adsorption, a new peak at 570 cm1 appeared on the infrared spectrum, which was thought to be the Cr = O bond formed by the Cr reaction [48].

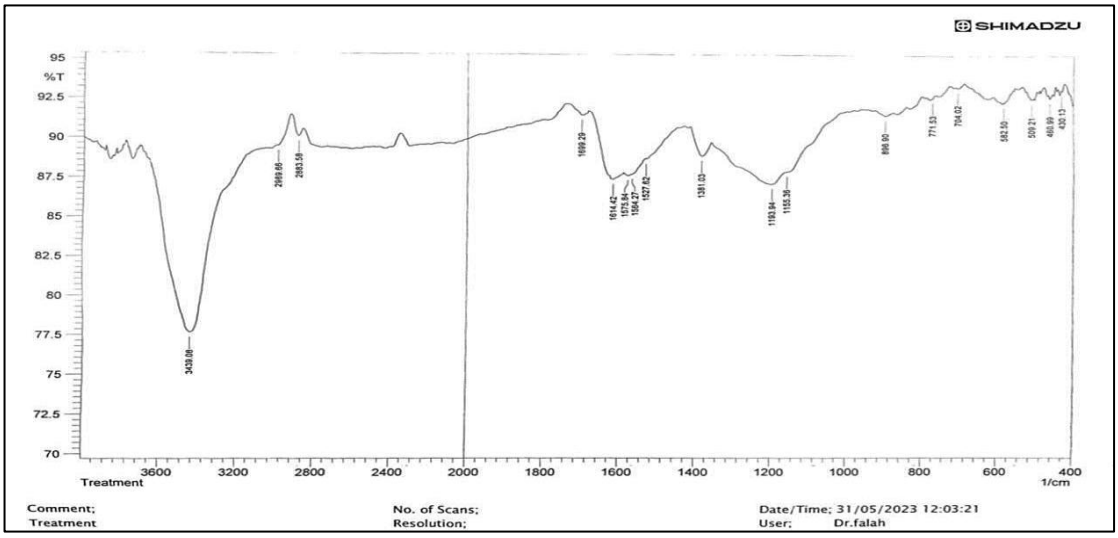

Figure (10): FTIR Analysis Peaks of Activated Date Pits after Cr (III)Adsorption.

8. Isotherm Modelling

The experimental results of the current study were designated with five adsorption isotherms to fix the mechanisms of heavy metal removal, Models like Freundlich, Langmuir, sips, tooth, and isothermal timkin.

8.1. Langmuir isotherm

A single layer of surface adsorption is described by the Langmuir model. Langmuir's notion is based on the idea that certain homogenous locations inside the adsorbent are where sorption takes place. The subsequent formula expresses the Langmuir model isotherm [49].

$$q_e = \frac{q_m\, b_l C_e}{1+b_l C_e} \qquad (3)$$

Where,

Ce: concentrations of contaminants in equilibrium state (mg L-1)

qe: contaminants uptake (mg g-1),

qm and bl; the maximum adsorption capacity (mg g-1) associated with Langmuir constant at equilibrium, and illustrates quantitatively the convergence among toxins and flocs (L mg-1)

8.2 Freundlich isotherm

The Freundlich model describes an equilibrium phase on heterogeneous surfaces but is incapable of predicting monolayer capacity. When combined with estimated results from experiments, Freundlich's submission is advantageous for a broad range of pollutant levels as well as suitable theoretical data requirements. It was employed in this study. The isotherm is associated with the equation below [50].

$$q_e = K_f C_e^{1/n} \qquad (4)$$

8.3 Sips isotherm

Sips model formed by combining Langmuir and Freundlich isotherms. The Freundlich isotherm is reduced as the adsorbate concentration decreases, while the Langmuir isotherm is increased as the adsorbate concentration increases [49].

$$q_e = \frac{k_s Ce^{\beta_s}}{1+a_s Ce^{\beta_s}} \qquad (5)$$

Ks: represent Sips model constant (L/g), β_S represent exponent of and α_S represent constant of Sips model (L/mg).

8.4 Toth isotherm

The tooth model depends on a potential concept of non-homogeneous absorption. This isotherm is appropriate with quasi-Gaussian energy dispersion. The main principle is that the site has adsorption power less than the maximum or peak adsorption power [51]. Subsequent calculation demonstrates the to the isotherm model.

$$q_e = \frac{q_m C_e}{(b+C_e^m)^{\frac{1}{m}}} \quad (6)$$

Where, b and m are the Toth isotherm constants.

8.5. Temkin isotherm

Temkin an isotherm explains the way the adsorption isotherm is affected by adsorption substances and adsorption interactions [52]. As coverage increases, the heat of adsorption is assumed to decrease linearly. The constant distribution of binding energies distinguishes this adsorption. The next formula illustrates the Temkin model [49]:

$$qe = BlnAT + BlnCe \quad (7)$$

$$B = \frac{RT}{bt} \quad (8)$$

Where B can be found from Equation (8) and is associated with the heat of sorption (J mol−1), AT represents optimum binding power (g−1), R is a gas constant (8.314 kJ mol−1), T stays the temperature (K), and bt represent the constant of the Temkin model, that fixes the adsorption potential of adsorbent [50]the isotherms for the adsorption of the cr(III) (qexp in contrast to Ce) by the ACDP are exposed in Figure 11. Table 2 to show the variables and correlation coefficient (R^2) results for the five models. Owing to the experimental outcomes proved, the cr (III) adsorption onto the ACDP is more fitted with the Sips model. Paid on the correlation factor (R^2) 0.9996, Adsorption utilizes the Sips isotherm model, which is superior to other isotherm models because it is a blend of the Langmuir and Freundlich models and can accommodate a wide range of solute concentrations. Furthermore, the Sips model specifies that both homogeneous and heterogeneous adsorptions occurred. The reactive cr (III) concentration changing from 0 to 75 mg/L had a calculated value of the separation factor (RL) between 0<RL<1. These results detected that adsorption is a spontaneous process.

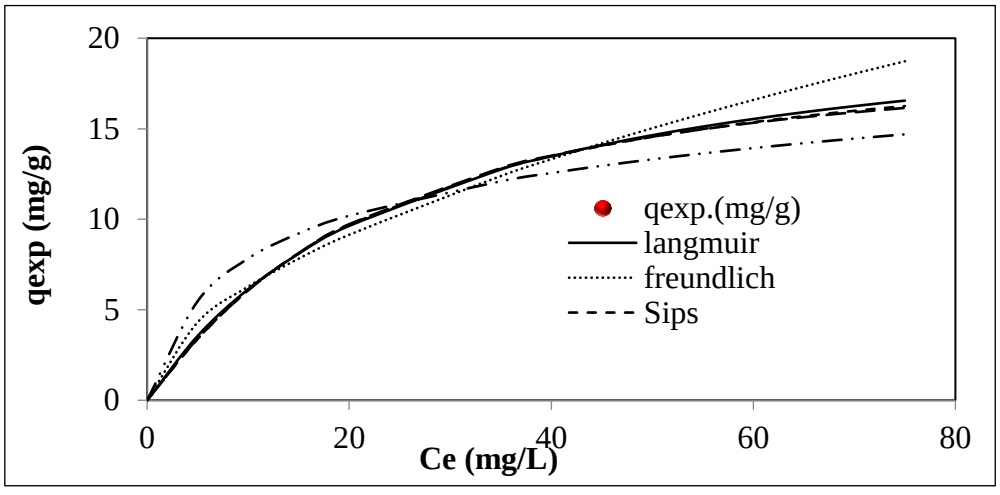

Figure (11): Adsorption isotherms of Cr (III)by the ACDP. Experimental environments: pH=6, dosage=0.5 g/100 mL Cr(III) solution, agitation speed= 250 rpm, connection time= 90 min, P.S=250 µm and temperature=25 °C

Table 2: Parameters of Each Model Used and Coefficients of Determination (R^2) for the Date Pits Waste Adsorbent.

Isotherm model	Eq.	Model parameters	Parameter value	R^2
Langmuir	$q_e = \frac{q_m\, b_l C_e}{1 + b_l C_e}$	q_m, mg/g	22.404	0.99913
		b, L/mg	0.0377	
Freundlich	$q_e = K_f C_e^{1/n}$	Kf	1.799866	0.986
		n	1.843246	
Sips	$q_e = \frac{k_s C e^{\beta_s}}{1 + a_s C e^{\beta_s}}$	KS	0.7052947	0.9996
		BS	1.088	
		as	0.034	
Toth	$q_e = \frac{q_m C_e}{(b + C_e^m)^{\frac{1}{m}}}$	q_{max}	19.4729	0.99954
		b	59.59	
		m	1.255	
Timkin	$q_e = BlnA_T + BlnC_e$	A_T	2.186	0.925
		B	3.4025	

9.Adsorption kinetics of cr(III)

To investigate the cr (III) adsorption mechanisms, the current study experiment used kinetic statistical studies with pseudo-first-order and pseudo-second-order models. Equation 9 [53] represents the pseudo-first-order model, and Table 3 shows the pseudo-first-order kinetics.

$$Ln(q_e - q_t) = ln\, q_e - k_1 t \qquad (9)$$

The slopes and intercepts of the ln(qe − qt) versus (vs) t (see Table 3) were used to determine the k_1 and qe parameters. Here, q_e (mg/g) denote adsorbate uptake at the equilibrium, q_t (mg/g) for the sorption uptake, and t (min) for the adsorp-tion time, k_l (l/min). Correlation coefficients (R^2) for the ACDP waste was 0.90 when the q_{exp} was 4.6 respectively. For the reason that adjusted R2 values is low and the significant consistency among the theoretical and experimental qe, exp data, The pseudo-first-order model did not accurately predict Cr adsorption onto ACDP adsorbent. Equation 10 corresponds to the pseudo-second-order model [54,55], and Table 3 lists its pseudo-second-order parameters. Table 3 summarizes the intercepts and curves identified on the t/qt vs t chart. According to the results, the adjusted R2 obtained was close to one. Moreover, the qe, cal evaluation agreed perfectly with the qe,exp results. The findings demonstrated that pseudo-second-order kinetics could be used to model the sorption of Cr onto ACDP waste.

$$\frac{t}{q_t} = \left(\frac{1}{k_2 q_e^2}\right) + \left(\frac{t}{q_t}\right) \quad (10)$$

where: qe (mg/g) represented adsorption uptake at equilibrium;

q_t: represents the adsorption capacity (mg/g).

t: represents adsorption time (min).

k_2: denotes a constant (mg/g·min).

Equation 11 suggests the intraparticle diffusion in this study. [56,57] Conversely, table 3 illustrates the kinetic figures of adsorption with varying time periods (0–90) min, C0 = 25 mg/L, pH = 6, ACDP waste dose = 0.5 g/L contaminant. solution, agitated speed = 250 rpm, and contaminant solution value temperature = 25 °C.

$$q_t = k_p t^{\frac{1}{2}} + C \quad (11)$$

where: C represents the intercepted amount (mg/g).
k_p is the intraparticle constant mass flow rate (mg/g·$min^{0.5}$).

Equivalent adjusted R^2 of intraparticle diffusion from the literature review is listed in Table 3. By outcomes, the pseudo-first-order molecular diffusion concept in the current investigation was unrelated to the adsorbate. The pseudo-second-order adsorption kinetics was able to achieve optimum adsorption with R^2 values of 0.98, 0.99, and 0.98 when Co = 25mg/L, which is a suitable match with the results obtained during the experiments period. Additionally, the results indicated an excellent fit between the adsorbed observations and the pseudo-second-order kinetics models, thereby verifying the model's chemisorption-based adsorbed assumption.

Table 3: Pseudo-first-order, Pseudo-second-order, and Intraparticle Diffusion Coefficient for Cr adsorption.

model	Parameter				
	q_{exp}	q_{cal}		R^2	
Pseudo-first order	4.6	6.18	K_1: 0.0449	0.900	
Pseudo-second order	4.6	6.005	K_2: 0.0053	0.972	
ntra-particle diffusion	4.6	4.679	K_p: 0.4769	0.991	C: 0.155

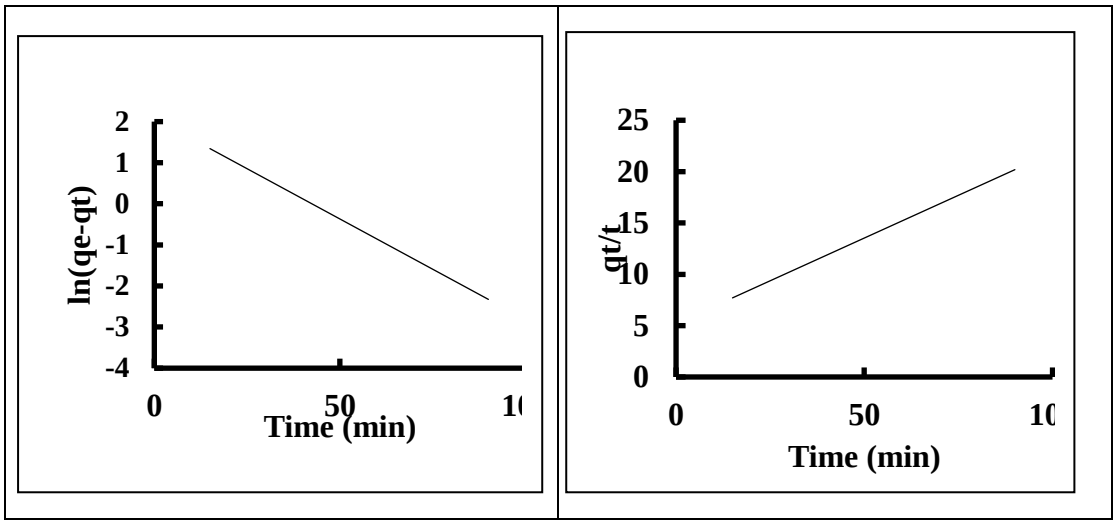

(a) (b)

Fig (12): (a) Pseudo-first-order, (b)Pseudo-second-order

Conclusions

The batch experiments' findings showed that several factors had a major impact on the chromium ions' interactions with the ACDP to achieve the highest removal percentage. These factors involved the beginning pollutant concentration, the initial pH, the dose of the sorbent, the rate of agitation, and the sorbent's particle size corresponding to 25 mg/l, 6, 2 g ACPD per 100 ml,250 rpm, and 250 µm respectively to remove 95% of Cr(III). Multiple types of sorption isotherm calculations were used to match the kinetic measurements for the sorption of chromium ions onto ACDP, the SIPS sorption isotherm proved to most closely approximate the data via a coefficient of determination (R2) of 0.996. Due to the good agreement between the fitted and experimental results, the data for the sorption of Cr (III) onto ACDP were found to obey the pseudo-second-order model, the most dominant mechanism in the sorption process was chemisorption.

References

[1] N. Sezgin, N. Balkaya, Adsorption of heavy metals from industrial wastewater by using polyacrylic acid hydrogel, Desal. Water. Treat., 57 (2016) 2466–2480.

[2] S. Ba, K. Ennaciri, A. Yaacoubi, A. Alagui, and A. Bacaoui, "Activated carbon from olive wastes as an adsorbent for chromium ions removal," *Iran. J. Chem. Chem. Eng.*, vol. 37, no. 6, pp. 107–123, 2018.

[3] Nieboer E.,.Shaw S.L., "Mutagenic and other Genotoxic Effects of Chromoim Compounds, in Chromium in the Natural and Human Environments", Eds Nriagu J.O., Nieboer E., (Wiley, New York), Chap. 16: 399-442 (1988).

[4] World Health Organization, Chromium Environmental Health Criteria 61. Geneva, Switzerland (1988).

[5] Gopi Krishna P., Mary Gladis J., Rambabu U., Prasada Rao T., Naidu G.R.K., Preconcentrative Separation of Chromium(VI) Species from Chromium(III) by Coprecipitation of its Ethyl Xanthate Complex onto Naphthalene, Talanta, 63: 541-546 (2004).

[6] Kongsricharoern N., Polprasert C., Chromium Removal by a Bipolar Electro-Chemical Precipitation Process, Water Sci. Technol., 34(9): 109-116 (1996).

[7] Ghanbari Pakdehi S., Adsorption of Cr(III) and Mg(II) from Hydrogen Peroxide Aqueous Solution by Amberlite IR-120 Synthetic Resin, Iran. J. Chem. Chem. Eng. (IJCCE), 32(2): 49-55 (2013).

[8] Ghanbari Pakdehi S., Adsorptive Removal of Al, Zn, Fe, Cr and Pb from Hydrogen Peroxide Solution by IR-120 Cation Exchange Resin, Iran. J. Chem. Chem. Eng. (IJCCE), 35(1): 75-84 (2016)

[9] Das C., Patel P., De S., DasGupta S., Treatment of Tanning Effluent Using Nanofiltration Followed by Reverse Osmosis, Sep. Purif. Technol., 50: 291- 299 (2006).

[10] Parinejad M., Yaftian M.R., A Study on the Removal of Chromium(VI) Oxanions from Acid Solutions by Using Oxonium Ion-Crown Ether Complexes as Mobile Carrier Agents, Iran. J. Chem. Chem. Eng. (IJCCE), 26(4): 19-27 (2007).

[11] Gaikwad M.S., Balomajumder C., Removal of Cr(VI) and Fluoride by Membrane Capacitive Deionization with Nanoporous and Microporous Limonia Acidissima (Wood Apple) Shell Activated Carbon Electrode, Sep. Purif. Technol., 195: 305-313 (2018).

[12] Liu J., Wang C., Shi J., Liu H., Tong Y., Aqueous Cr(VI) Reduction by Electrodeposited ZeroValent Iron at Neutral pH: Acceleration by Organic Matters, J. Hazard. Mater., 163: 370-375 (2009).

[13] Meunier N., Drogui P., Montane C., Hausler R., Mercier G., Blais J.F. Comparison between Electrocoagulation and Chemical Precipitation for Metals Removal from Acidic Soils Leachate, J. Hazard. Mater., 137: 581–590 (2006).

[14] Wang F., Xie Z., Xie L., Preparation of Polyamide Microcapscules and their Application Treating Industrial Wastewater Containing Cr6+ , Chem. Res., 13: 36–38 (2002).

[15] Abdel-Halim E.S., Al-Deyab S.S., Hydrogel from Cross Linked Polyacrylamide/guar Gum Graft Copolymer for Sorption of Hexavalent Chromium Ion, Carbohydr. Polym., 86(3): 1306-1312 (2011).

[16] Samani M.R., Borghei S.M., Olad A., Chaichi M.J., Influence of Polyaniline Synthesis Conditions on its Capability for Removal and Recovery of Chromium from Aqueous Solution, Iran. J. Chem. Chem. Eng. (IJCCE), 30 (3): 97-100 (2011).

[17] Arfaoui S., Frini-Srasra N., Srasra E., Modelling of the Adsorption of the Chromium Ion by Modified Clays, Desalination, 222: 474–481 (2008).

[18] Benhammou A., Yaacoubi A., Nibou L., Tanouti B., Chromium(VI) Adsorption from Aqueous Solution onto Moroccan Al-Pillared and Cationic Surfactant Stevensite, J. Hazard. Mater., 140: 104–109 (2007).

[19] Yavuz A.G., Dincturk-Atalay E., Uygun A., Gode F., Aslan E., A Comparison Study of Adsorption of Cr(VI) from Aqueous Solutions Onto AlkylSubstituted Polyaniline/Chitosan Composites, Desalination, 279: 325–331 (2011).

[20] Gupta V.K., Rastogi A., Nayak A., Adsorption Studies on the Removal of Hexavalent Chromium from Aqueous Solution Using a Low Cost Fertilizer Industry Waste Material, J. Colloid Interf. Sci. 342: 135–141 (2010).

[21] Jung C., Heo J., Han J., Her N., Lee S.J, Ohd J., Ryud J., Yoon Y., Hexavalent Chromium Removal by Various Adsorbents: Powdered Activated Carbon, Chitosan, and Single/Multi-Walled Carbon Nanotubes, Sep. Purif. Technol., 106: 63–71 (2013).

[22] Uysal M., Ar I., Removal of Cr(VI) from Industrial Wastewaters by Adsorption Part I: Determination of Optimum Conditions, J. Hazard. Mater., 149: 482– 491 (2007).

[23] Di Natale F., Lancia A., Molino A., Musmarra D., Removal of Chromium Ions form Aqueous Solutions by Adsorption on Activated Carbon and Char, J. Hazard. Mater., 145: 381–390 (2007).

[24] González Bermúdeza Y., Ricoa I.L.R., Guibal E., Calero de Hocesc M., Martín-Larac M.Á., Biosorption of Hexavalent Chromium from Aqueous Solution by Sargassum muticum Brown Alga. Application of Statistical Design for Process Optimization, Chem. Eng. J., 183: 68–76 (2012).

[25] Faghihian H., Rasekh M., Removal of Chromate from Aqueous Solution by a Novel Clinoptilolite Polyanillin Composite, Iran. J. Chem. Chem. Eng. (IJCCE), 33 (1): 45-51 (2014).

[26] Owlad M., Aroua M.K., Wan Daud W.M.A., Hexavalent Chromium Adsorption on Impregnated Palm Shell Activated Carbon with Polyethyleneimine, Bioresour. Technol. 101: 5098–5103 (2010).

[27] Zhang H., Tang Y., Cai D., Liu X., Wang X., Huang Q., Yu Z., Hexavalent Chromium Removal from Aqueous Solution by Algal Bloom Residue Derived Activated Carbon: Equilibrium and Kinetic Studies, J. Hazard. Mater., 181: 801–808 (2010).

[28] Gupta V.K., Nayak A., Agarwal S., Bioadsorbents for Remediation of Heavy Metals: Current Status and Their Future Prospects, Review Article, Environ. Eng. Res., 20(1): 001-018 (2015).

[29] Duran U., Coronado-Apodaca K.G., Meza-Escalante E.R., Ulloa-Mercado G., Serrano D., Two Combined Mechanisms Responsible to Hexavalent Chromium Removal on Active Anaerobic Granular Consortium, Chemosphere, 198: 191-197 (2018).

[30] Rosales E., Meijide J., Pazos M., Sanromán M. A., Challenges and Recent Advances in Biochar as Low-Cost Biosorbent: From Batch Assays to Continuous-Flow Systems, Bioresour. Technol, 246: 176–192 (2017).

[31] Zhang X., Zhang L., Li A., Eucalyptus Sawdust Derived Biochar Generated by Combining the Hydrothermal Carbonization and Low Concentration KOH Modification for Hexavalent Chromium Removal, J Environ Manage., 206: 989- 998 (2018).

[32] Su H., Chong Y., Wang J., Long D., Qiao W., Ling L., Nanocrystalline Celluloses-Assisted Preparation of Hierarchical Carbon Monoliths for Hexavalent Chromium Removal, J. Colloid Interface Sci., 510: 77–85 (2018).

[33] Burakov A.E., Galunin E.V., Burakova I.V., Kucherova A.E., Agarwal S., Tkachev A.G., Gupta V.K., Adsorption of Heavy Metals on Conventional and Nanostructured Materials for Wastewater Treatment Purposes: A Review, Ecotoxicol Environ Saf., 148: 702–712 (2018).

[34] E. Vunain, J. B. Njewa, T. T. Biswick, and A. K. Ipadeola, “Adsorption of chromium ions from tannery effluents onto activated carbon prepared from rice husk and potato peel by H3PO4 activation,” *Appl. Water Sci.*, vol. 11, no. 9, pp. 1–14, 2021, doi: 10.1007/s13201-021-01477-3.

[35] H. M. Rashid and A. A. H. Faisal, “Removal of Dissolved Trivalent Chromium Ions from Contaminated Wastewater using Locally Available Raw Scrap Iron-Aluminum Waste,” *Al-Khwarizmi Eng. J.*, vol. 15, no. 1, pp. 134–143, 2019, doi: 10.22153/kej.2019.06.005

[36] K. K. Wong, C. K. Lee, K. S. Low, and M. J. Haron, “Removal of Cu and Pb by tartaric acid modified rice husk from aqueous solutions,” *Chemosphere*, vol. 50, no. 1, pp. 23–28, 2003, doi: 10.1016/S00456535(02)00598-2.

[37] Z. S. Nassir, “RTIFICIAL NEURAL NETWORK (ANN) APPROACH FOR MODELING OF HEAVY METALS ADSORPTION FROM AQUEOUS SOLUTION BY LOW COST ADSORBENTS”,

M.S.thesis ,Univ.of Baghdad ,Baghdad ,Iraq ,2016.

[38] P. V Nidheesh, G. Divyapriya, F. E. Titchou, and M. Hamdani, "Treatment of textile wastewater by sulfate radical based advanced oxidation processes," *Sep. Purif. Technol.*, vol. 293, p. 121115, 2022.

[39] A. H. Sadek and M. K. Mostafa, "Preparation of nano zero-valent aluminum for one-step removal of methylene blue from aqueous solutions: cost analysis for scaling-up and artificial intelligence," *Appl. WaterSci.*, vol. 13, no. 2, pp. 1–23, 2023, doi: 10.1007/s13201-022-01837-7.

[40] M. Azam, S. M. Wabaidur, M. R. Khan, M. S. Islam, and S. I. Al-Resayes, "Removal of chromium(III) andc admium(II) heavy metal ions from aqueous solutions using treated date seeds: An eco-friendly method," *Molecules*, vol. 26, no. 12, 2021, doi: 10.3390/molecules26123718.

[41] M. F. F. Sze and G. McKay, "An adsorption diffusion model for removal of para-chlorophenol by activated carbon derived from bituminous coal," *Environ. Pollut.*, vol. 158, no. 5, pp. 1669–1674, 2010, doi: 10.1016/j.envpol.2009.12.003.

[42] J. W. Brault, "New approach to high-precision Fourier transform spectrometer design," *Appl. Opt.*, vol. 35, no. 16, pp. 2891–2896, 1996.

[43] K. Mahmoudi, K. Hosni, N. Hamdi, and E. Srasra, "Kinetics and equilibrium studies on removal of methylene blue and methyl orange by adsorption onto activated carbon prepared from date pits-A comparative study," *Korean J. Chem. Eng.*, vol. 32, no. 2, pp. 274–283, 2015.

[44] I. M. Iloamaeke and C. O. Julius, "Treatment of Pharmaceutical Effluent Using seed of Phoenix Dactylifera as a Natural Coagulant," *J. Basic Phys. Res.*, vol. 9, no. 1, pp. 91–100, 2019.

[45] A. Benbiyi, M. El Guendouzi, S. Kouniba, and A. Zourif, "Response Surface Modeling for Malachite Green Removal Using the Box-Behnken Experimental Design," *Environ. Ecol. Res.*, vol. 10, no. 6, pp. 830–838, 2022, doi: 10.13189/eer.2022.100617.

[46] J. M. Salman and F. M. Abid, "Preparation of mesoporous activated carbon from palm-date pits: optimization study on removal of bentazon, carbofuran, and 2, 4-D using response surface methodology," Water Sci. Technol., vol. 68, no. 7, pp. 1503–1511, 2013.

[47] M. A. Islam, I. A. W. Tan, A. Benhouria, M. Asif, and B. H. Hameed, "Mesoporous and adsorptive properties of palm date seed activated carbon prepared via sequential hydrothermal carbonization and sodium hydroxide activation," Chem. Eng. J., vol. 270, pp. 187–195, 2015.

[48] Y. Shu *et al.*, "Almond shell-derived, biochar-supported, nano-zero-valent iron composite for aqueous hexavalent chromium removal: performance and mechanisms," *Nanomaterials*, vol. 10, no. 2, p. 198, 2020.

[49] S. J. Mohammed, M. J. M-Ridha, K. M. Abed, and A. A. M. Elgharbawy, "Removal of levofloxacin and ciprofloxacin from aqueous solutions and an economic evaluation using the electrocoagulation process," Int. J. Environ. Anal. Chem., vol. 00, no. 00, pp. 1–19, 2021, doi: 10.1080/03067319.2021.1913733.

[50] H. S. Alhares et al., "Sunflower Husks Coated with Copper Oxide Nanoparticles for Reactive Blue 49 and Reactive Red 195 Removals: Adsorption Mechanisms, Thermodynamic, Kinetic, and Isotherm Studies," Water. Air. Soil Pollut., vol. 234, no. 1, 2023, doi: 10.1007/s11270-022-06033-6.

[51] Y.A. Ouaissa, M. Chabani, A. Amrane and A. Bensmaili, J. Environ. Chem. Eng. 2 (1), 177 (2014). doi:10.1016/j.jece.2013.12.009

[52] M. Al-Shannag, Z. Al-Qodah, K. Bani-Melhem, M. R. Qtaishat, and M. Alkasrawi, "Heavy metal ions removal from metal plating wastewater using electrocoagulation: Kinetic study and process performance," *Chem. Eng. J.*, vol. 260, pp. 749–756, 2015, doi: 10.1016/j.cej.2014.09.035

[53] S. T. Akar, A. Gorgulu, Z. Kaynak, B. Anilan, and T. Akar, "Biosorption of Reactive Blue 49 dye under batch and continuous mode using a mixed biosorbent of macro-fungus Agaricus bisporus and Thuja orientalis cones," *Chem. Eng. J.*, vol. 148, no. 1, pp. 26–34, 2009, doi: 10.1016/j.cej.2008.07.027.

[54] M. Asgher and H. N. Bhatti, "Removal of reactive blue 19 and reactive blue 49 textile dyes by citrus waste biomass from aqueous solution: Equilibrium and kinetic study," *Can. J. Chem. Eng.*, vol. 90, no. 2, pp. 412–419, 2012, doi: 10.1002/cjce.20531.

[55] M. Salman, H. Alhares, Q. Ali, M. M-Ridha, S. Mohammed, and K. M. Abed, "Cladophora Algae Modified with CuO Nanoparticles for Tetracycline Removal from Aqueous Solutions," *Water, Air, Soil Pollut.*, vol. 233, Aug. 2022, doi: 10.1007/s11270-022-05813-

[56] Z. Belala, M. Jeguirim, M. Belhachemi, F. Addoun, and G. Trouvé, "Biosorption of basic dye from aqueous solutions by Date Stones and Palm-Trees Waste: Kinetic, equilibrium and thermodynamic studies," *Desalination*, vol. 271, no. 1–3, pp. 80–87, 2011, doi: 10.1016/j.desal.2010.12.009.

[57] M-Ridha, M.J., Faeq Ali, M., Hussein Taly, A., Abed, K.M., Mohammed, S.J., Muhamad, M.H., Abu Hasan, H., 2022. Subsurface Flow Phytoremediation Using Barley Plants for Water Recovery from Kerosene-Contaminated Water: Effect of Kerosene Concentration and Removal Kinetics. Water 14, 687. https://doi.org/10.3390/w14050687